Use of Fe_3O_4 nanoparticles in reactor co-digestion of residues from 1G2G ethanol biorefinery: microbiological routes and operational aspects

Maria Paula. C. Volpi*[a,b], Gustavo Mockaitis[b], Guillaume Bruant[c], Julien Tremblay[c], Bruna S. Moraes[a]

[a]Interdisciplinary Center of Energy Planning, University of Campinas (NIPE/UNICAMP), R. Cora Coralina, 330 - Cidade Universitária, Campinas - SP, 13083-896, Brazil.

[b]Interdisciplinary Research Group on Biotechnology Applied to the Agriculture and the Environment (GBMA), School of Agricultural Engineering (FEAGRI), University of Campinas (UNICAMP), Av. Candido Rondon, 501 - Cidade Universitária, Campinas - SP, 13083-875, Brazil.

[c] Energy, Mining and Environment Research Centre, National Research Council of Canada, 6100 Royalmount Ave., Montreal, H4P 2R2, QC, Canada

*Corresponding author: mcardealvolpi@gmail.com; phone (+55) 19 98367-2506

ABSTRACT

The co-digestion of residues from the sugarcane industry has already proven to be a highly attractive process for biogas production through anaerobic digestion (AD). The use of residues such as vinasse (1G) filter cake (1G) and deacetylation liquor (2G) in operation in a continuous CSTR reactor showed a possibility of integration of 1G and 2G ethanol biorefineries through AD in previous work by our research group. The use of nanoparticles (NP) is a favorable way to optimize AD processes, as these additives serve as a means of introducing nutrients into the process in a more assertive way from the point of view of distribution and interaction with microorganisms. In this context, the present work proposed the optimization of the co-digestion of vinasse, filter cake, and deacetylation liquor in a continuous reactor through the addition of Fe_3O_4 NP, by the purpose of comparison results with the operation of the same substrates and the same condition but without NP. Initially, tests were carried out in batches with different concentrations of NPs, to evaluate the best concentration to be added in the continuous reactor. A concentration of 5 mg L^{-1} was chosen, and it was added to each increase in organic rate load (ORL) used in the process. CH_4 production reached maximum values of 2.8 ± 0.1 $NLCH_4$ gVS^{-1} and organic matter removal 71 ± 0.9%, in phase VI, with ORL of 5.5 gVS L^{-1} day^{-1}. This production was 90% higher than the reactor co-digestion operation without the presence of NP. Furthermore, according to the results of pH, alkalinity, it can be concluded that the methanogenesis stabilized at 60 days of operation, being 30 days before when there was no NP added. The development of AD was stable, with low variations in the oxidation-reduction potential (ORP) and with stable organic acid (OA) concentrations, indicating the possibility of route propionic acid to produce CH_4. The main methanogenic *Archeae* found was *Methanoculleus*, indicating that the predominant metabolic route was that of syntrophic acetate oxidation (SAO) coupled with hydrogenotrophic methanogenesis. The use of Fe_3O_4 NP managed to improve the AD operation of residues from the 1G2G ethanol production industry and did not modify the microbial community present, only stimulated their growth.

Keywords: Nanoparticles; Co-digestion; Methane optimization; 1G2G ethanol residues

1. INTRODUCTION

Anaerobic digestion (AD) is a process of managing liquid and solid waste that allows energy recovery through methane (CH_4) (Deublin and Steinhauser, 2008). This technique is used for different types of residues, and the literature has shown the great potential for CH_4 generation from sugarcane residues, especially vinasse (Djalma Nunes Ferraz Júnior et al., 2016; Fuess et al., 2017; Moraes et al., 2015).

Within this context, anaerobic co-digestion emerged to improve biogas production. Co-digestion is characterized by the AD of two or more substrates which is an option to overcome the disadvantages of mono-digestion, mainly concerning the balance of nutrients and to improve the economic viability of AD plants (Hagos et al., 2017). Co-digestion has the advantages of optimizing CH_4 production, in addition to better stabilizing the process. With the presence of different substrates, it is possible to provide synergistic effects within the reactor, increasing a load of biodegradable compounds (Hagos et al., 2017).

Promoting the co-digestion of residues from the sugarcane industry can be an alternative to improve the management of the various residues obtained in this biorefinery, in addition to increasing CH_4 generation. Beyond vinasse, the filter cake is a lignocellulosic residue obtained from ethanol production that has a high potential for biogas production (Volpi et al., 2021a)(Janke et al., 2016) and can potentiate the vinasse CH_4 production by co-digesting these two residues (Volpi et al., 2021a). However, the literature reports little about the use of residues from the production of 2G ethanol for AD, mainly emphasizing the use of only 2G vinasse (Moraes et al., 2014) but not reporting the use of liquors that can also be obtained from the 2G ethanol production process. In the work of Brenelli et al. (Brenelli et al., 2020), an alkaline pretreatment of sugarcane straw was performed to be used in the production of 2G ethanol. Within this

process, straw deacetylation was carried out before the hydrothermal pretreatment, since the straw hemicellulose is highly acetylated. The residue generated from this process, called deacetylation liquor, is rich in volatile fatty acids such as acetic acid, formic acid, being promising for CH_4 production through AD, or co-digestion (Volpi et al., 2021a).

In previous works by our research group, it was proposed to co-digest the residues of the sugarcane industry for the production of biogas, to promote the integration of the 1G2G ethanol biorefinery. The results showed that the co-digestion of vinasse, filter cake, and deacetylation liquor in semi-Continuous Stirred Tank Reactor (s-CSTR) reached production of 230 $NmLCH_4\ gSV^{-1}$ and organic matter removal efficiency 83% ± 13 , showing that the co-digestion of the proposed residues, increased the production of CH_4, about mono-digestion of vinasse (Volpi et al, 2021b).

To increase the production of CH_4 in operation in reactors, the literature reports that the use of additives can improve its performance, mainly related to the use of micronutrients (Demirel and Scherer, 2008). Scherer et al. (Scherer et al., 1983) classified that for methanogenic organisms the importance of micronutrients is given in the following order: Fe >> Zn> Ni> Cu = Co = Mo> Mn, indicating that such elements have essential roles as in the construction of methanogenic cells. Besides this, many of these micronutrients have concentrations that must be met, as cell growth may be limited or inhibited. Zhang et al. (Zhang et al., 2003) showed that for Co, Ni, Fe, Zn, Cu if the concentrations are less than 4.8, 1.32, 1.13, 0.12 g L^{-1} respectively, there is a limitation of the growing culture of methanogenic microorganisms in terms of cell density.

Among the different trace elements, Fe is important to stimulate the formation of citrocomes and ferredoxins, important for cellular energy metabolism, mainly of methanogenic archaea (Choong et al., 2016). In addition to methanogenesis, Fe is also important to catalyze chemical reactions of some metalloenzymes used in acetogenesis,

such as dehydrogenase format, carbon monoxide dehydrogenase (Choong et al., 2016). The hydrolysis and acidification phase of AD is also benefited by Fe as a growth factor since Fe supplementation can accelerate these steps (Yu et al., 2015).

In the work of Demirel and Scherer (Demirel and Scherer, 2011), the addition of Fe_3O_4 improved the production of biogas and the CH_4 content in biogas using cow dung and chicken litter. And Zhang et. (Zhang et al., 2011) al showed that Zerovalent Iron (ZVI) helps to create an improved anaerobic environment for wastewater treatment and that promotes the growth of methanogens with greater removal of chemical oxygen demand (COD).

One of the ways to promote this addition of components to optimize AD is through the use of nanoparticles (NPs). Nanotechnology allows the manipulation of matter on a nanoscale (1 to 100 nm), and NPs are materials found in this size range (Abdelsalam et al., 2016). The nano-size is important because it allows greater mobility of the active compound in the environment, in addition to allowing interaction with the biological system, facilitating the passage of the compound in cell membranes, absorption, and distribution in the metabolism. This happens due to its mesoscopic effect, small object effect, quantum size effect, and surface effect and to have the greater surface area and dispersibility (Abdelsalam et al., 2017a, 2017b, 2016).

Some authors have already studied the use of different nanoparticles to optimize the production of biogas in different types of waste. Henssein et al. (Hassanein et al., 2019) studied the use of NPs in AD of poultry litter. They observed that the production of CH_4 increased with the addition of NPs, being the NP concentrations (in mg L^{-1}) of 12 Ni (38.4% increase), 5.4 Co (29.7% increase), 100 Fe (29.1% increase), and 15 Fe_3O_4 (27.5% increase). Mu et al. (Mu et al., 2011a) studied the effect of metal oxide nanoparticles (nano-TiO2, nano-Al2O3, nano-SiO2, and nano-ZnO) on AD using

activated sludge as a substrate, and the results showed that only Nano-ZnO had an inhibitory effect on CH_4 production in concentrations starting at 30 mg g^{-1}- total suspended solids (TSS). Abdeslam et al. (Abdelsalam et al., 2016) used the metallic NPs Co, Ni, Fe, and Fe_3O_4 to compare the production of biogas and CH_4 from the anaerobic digestion of cattle manure and they obtained as a result that the methane yield increased significantly ($p < 0.05$) 2, 2.17, 1.67 and 2.16 times about the control, respectively. Wang et al. (Wang et al., 2016) investigated the effects of representative NPs, (nZVI, Fe_2O_3 NPs) on CH_4 production during the anaerobic digestion of waste activated sludge, and the concentration of 10 mg g^{-1} TSS nZVI and 100 mg g^{-1} TSS Fe_2O_3 NPs increased methane production to 120% and 117% of the control, respectively. The literature has shown that experiments with Fe_3O_4, which are magnetic NPs, improved the AD process due to their characteristics of superparamagnetic, high coercivity, and low Curie temperature. In addition to these characteristics, Fe_3O_4 NPs are also non-toxic and biocompatible (Abdelsalam et al., 2017b; Mamani and Gamarra, 2014), which may favor AD processes.

To date, studies on the use of NPs to optimize the production of biogas in co-digestion with residues from the sugarcane industry have not been found in the literature. In our previous work (Volpi et al., 2021b) co-digestion of residues from the sugarcane industry and characterization of the microbial community was carried out. To promote optimization of the process, the objective of the present study was to co-digest vinasse, filter cake, and deacetylation liquor in an s-CSTR reactor, with the addition of Fe_3O_4 nanoparticles. First, biochemical Methane Potential (BMP) assays were performed with different concentrations of Fe_3O_4 NPs, to assess what would be the best concentration to use in the reactor, and after that, the operation in the reactor was performed, with a characterization of the microbial community before the reactor and after leaving the reactor, to compare the process with adding NPs in changing the microbial community.

2. MATERIAL AND METHODS

2.1 Residues and Inoculum

The substrates were vinasse and filter cake from Iracema sugarcane mill (São Martinho group, Iracemápolis, São Paulo state, Brazil) and the liquor from the straw pretreatment process, performed at the National Biorenovables Laboratory (LNBR) from the Brazilian Center for Research in Energy and Materials (CNPEM). Deacetylation pre-treatment was applied to sugarcane straw on a bench-scale as described in Brenelli et al. (Brenelli et al., 2020). The anaerobic consortium of the mesophilic reactor (BIOPAC®ICX - Paques) from the aforementioned Iracema mill was used as inoculum. The substrates were characterized in terms of series of solids, volatile solids (VS) and total solids (TS) through method 2540 and pH (pHmeter PG 1800), according to Standard Methods - APHA (APHA, AWWA, 2012), Organic acids (OA), alcohol, carbohydrates, in High-Performance Liquid Chromatography (HPLC, Shimadzu®). The HPLC consisted of a pump-equipped apparatus (LC-10ADVP), automatic sampler (SIL-20A HT), CTO-20A column at 43 °C, (SDP-M10 AVP), and Aminex HPX-87H column (300 mm, 7.8 mm, BioRad). The mobile phase was H_2SO_4 (0.01 N) at 0.5 ml $min^{-1.}$ The inoculum was characterized in terms of VS and TS. The inoculum presented 0.0076 ± 0.00 g mL^{-1} in terms of VS and 0.0146 ± 0.00 in terms of TS. The vinasse presented 0.014 ± 0.00 g mL^{-1} of VS and 0.0176 ± 0.00 g mL^{-1} of TS, the deacetylation liquor 0.0123 ± 0.00 g mL^{-1} of VS and 0.0219 ± 0.00 g mL^{-1} of TS, and filter cake 0.5454 ± 0.53 g mL^{-1} of VS and 0.6197 ± 0.54 g mL^{-1} of TS. The pH of the inoculum was 8.57 ± 0.14, the pH of vinasse was 4.25 ± 0.17 and the deacetylation liquor the pH was 9.86 ± 0.15. The elemental composition was performed for the characterization of filter cake in the Elementary Carbon, Nitrogen, Hydrogen and Sulfur Analyzer equipment (Brand:

Elementar; Model: Vario MACRO Cube - Hanau, Germany), was obtained 1.88% of N, 31.07% of C, 6.56% of H and 0.3% of S, all in terms of TS.

The results of OA, alcohol, and carbohydrates for liquid residues are presented in Table 1.

Table 1. Characterization of OA, carbohydrates, and alcohols of liquids residues

Compounds	Vinasse (mg L^{-1})	Deacetylation Liquor (mg L^{-1})
Acetate	1268.41	3250.00
Formate	--	650.00
Lactate	3706.94	423.18
Propionate	634.85	368.29
Butyrate	--	250.02
Isovalerate	931.63	269.03
Glucose	809.05	546.23
Methanol	8674.83	--

--: not carried out

2.2 Batch Tests

Batch tests were performed on the co-digestion of residues (vinasse + filter cake + deacetylation liquor in the proportion of 70:20:10 (in terms of VS) respectively following previous work (Volpi et al., 2021b) with different concentrations of Fe_3O_4 NPs to identify the best concentration to be used in the s-CSTR reactor. The tests were conducted in 250 ml Duran flasks, under 55 ° C, in which the inoculum was acclimated initially. On the first day, the temperature was increased to 40°C, then to 45°C and in 4 days it had reached 55°C. After reaching this temperature, the inoculum was kept for 1

week at 55°C, then from the beginning of the experiments. The experiments were in triplicate, with a 2:1 inoculum to substrate ratio (in terms of VS) added to each flask, following the protocol of Triolo et al. (Triolo et al., 2012) and the VDI 4630 methodology (VDI 4630, 2006). The pH of solution flasks was corrected to neutrality by adding solutions of NaOH (0.5 M) or H_2SO_4 (1 M) when necessary. N_2 has flowed into the headspace of each vial. The biogas produced was collected from the headspace with the Gastight Hamilton Super Syringe (1L) syringe through the flasks' rubber septum. Gas chromatography analyzes were also carried out to detect the concentration of CH_4 produced in the gas chromatograph (Construmaq MOD. U-13 São Carlos). The carrier gas was hydrogen (H2) gas (30 cm s-1) and the injection volume was 3 mL. The GC Column was made of 3-meter long stainless steel, 1/8 ”in diameter, and packaged with Molecular Tamper 5A for separation of O_2 and N_2 and CH_4 in the thermal conductivity detector (TCD). Digestion was terminated when the daily production of biogas per batch was less than 1% of the accumulated gas production. After the assay, the values were corrected for standard temperature and pressure (STP) conditions (273 K, 1.013 hPa).

The different concentrations of Fe_3O_4 NP used in each bottle are described in Table 2. The choice of concentrations was made based on studies with NP and AD that the literature shows (Abdelsalam et al., 2016; Wang et al., 2016). It is worth mentioning that a control flask was made (Flaks 1-Table2), adding only the inoculum and co-digestion, without NPs, to compare with the other bottles that contained NPs, and to evaluate the optimization of the process. Analysis of variance (ANOVA) was used to identify the existence of significant differences between the treatments ($p < 0.05$).

Table 2. Design of experiments of BMP

Flaks	Name in Graph	Fe_3O_4 NP Concentration (mg L^{-1})
1- Inoculum + Co-digestion	Control	0
2- Inoculum + Co-digestion + NP	NP 1	1
3- Inoculum + Co-digestion + NP	NP 2	5
4- Inoculum + Co-digestion + NP	NP 3	10
5- Inoculum + Co-digestion + NP	NP 4	20

2.3 Semi-continuous reactor: description and operation

The s-CSTR operation was followed according to previous work by our research group (Volpi et al., 2021b). 5L-Duran flask with 4L-working volume kept under agitation at 150 rpm by using an orbital shaking table Marconi MA 140. The operating temperature was 55°C, maintained by recirculating hot water through a serpentine. The reactor was fed once a day with the blend of co-substrates (in terms of volatile solids, VS): 70% of vinasse, 20% of filter cake, and 10% of deacetylation liquor, totaling 33.45 gVS L^{-1}. Throughout the operation, the Organics Loads Rate (OLR) was increased to use the maximum OLR without collapsing the reactor. At the beginning of the operation, Fe_3O_4 NP was added and when the reactor stabilized the CH_4 production, the OLR was increased, expected to stabilize the CH_4 production again and added the same concentration of Fe_3O_4 NPs. This was done for all OLRs (excepted for the last one). Table 3 presents the values of operational parameters applied to the s-CSTR according to the respective operation phases and the days that were added Fe_3O_4 NPs.

Table 3. Phases of reactor operation and the respective applied ORLs, feeding rate flows, and HRT.

Phase in Graph	OLR (gVS L^{-1} day^{-1})	Feeding rate (L day^{-1})	HRT (days)	NP Addition Day
I	2	0.250	16	24
II	2.35	0.285	14	47
III	3	0.363	11	72
IV	4	0.500	8	95
V	4.70	0.571	7	109
VI	5.5	0.666	6	123
VII	6.6	0.800	5	136
VIII	8	1.000	4	150
IX	9	1.140	3.5	--

Note: --: not added

2.3.1 s-CSTR monitoring analyzes

The volume of biogas produced was measured through the Ritter gas meter, Germany. The CH_4 content was determined by gas chromatography (Construmaq-MOD U-13, São Carlos) five times a week. OA, carbohydrates, alcohols, and organic matter content (in terms of VS) in the digestate were monitored following the same methodology described in the characterization of residues (section 2.1). The alkalinity from digestate also was determined using the titration method APHA, (APHA, AWWA, 2012). The pH and the Oxidation-reduction potential (ORP) of digestate were measured, immediately after sampling (before feeding) using a specific electrode for Digimed ORP. The pH was monitored also in the feed. All reactor monitoring analyzes followed as described in Volpi et al. (2021b).

2.4 Biology Molecular Analysis

Identification of the microbial community of the inoculum was carried out before being inserted in the reactor- Sample A1, and after the production of CH_4 was stabilized in the OLR of 4 gVS L^{-1} day^{-1} (Sample A2), to evaluate the change of the microbial community with the changes of the metabolic routes for the production of CH_4 and with the addition of Fe_3O_4 NP. The extraction and quantification and sequencing protocol were followed as described in Volpi et al. (2021b). Raw sequences were deposited in BioSample NCBI under accession number BioProject ID PRJNA781620.

2.5 NP preparations and characterization

Fe_3O_4 NP was used, due to the better performance of these NP in AD according to the literature (Abdelsalam et al., 2016; Ali et al., 2017; Zhang et al., 2020). The Fe_3O_4 NP used were IRON (II, III) OXIDE, NANOPOWDER, 50-100 N-SIGMA-ALDRICH. They were then diluted in distilled water at pH 7, in a glass bottle. Sodium dodecylbenzene sulfonate (SDS) at 0.1mM was used as a dispersing reagent to ensure NPs dispersion before use, as SDS has been shown to not significantly affect CH_4 production (Hassanein et al., 2019; Wang et al., 2016). To characterize the size of these NPs was performed analysis on the Laser Diffraction Particle Size Analyzer - MASTERSIZER-3000 (MALVERN INSTRUMENTS- MAZ3000-Worcestershire, U.K.). Measurement made in Wet Mode - HIDRO EV. The mathematical model employed: Mie. It considers that the particles are spherical and that they are not opaque - thus taking into account the diffraction and diffusion of light in the particle and the medium. They were made for samples of pure NP.

3. RESULTS AND DISCUSSION

3.1 Characterization of Fe_3O_4 NP

Figure 1 shows the size and distribution of Fe_3O_4 NP diluted in water pH 7. Figure 1a shows two populations, one up to nano size (0.1 µm) and the other that starts from 0.3 µm and is no considered a nanoparticle.

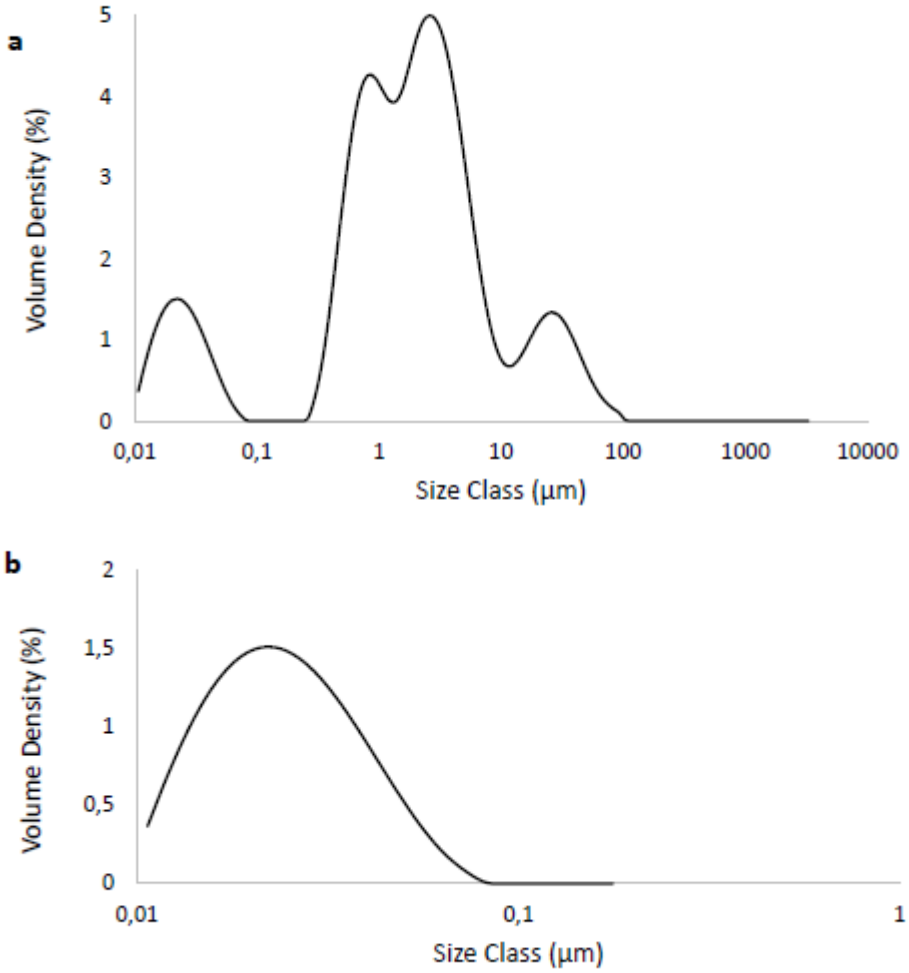

Figure 1. Size of Fe_3O_4 Nanoparticles (NP): (a): Involving all particles in the sample; (b) Nanosize cut of the particles

These results show that the sample used also contained particles larger than nanoparticles. The average size, including the two populations, was 180 ± 0.05 nm. This behavior of larger sizes found for Fe_3O_4 NP was also reported by Hansein et al. (Hassanein et al., 2019) who found sizes between 96-400 nm. In the work by Abdsalam et al.(Abdelsalam et al., 2017b), Fe_3O_4 NP sizes did not exceed 7 ± 0.2 nm. It is worth

mentioning that the NPs used by Abdsalam et al. (Abdelsalam et al., 2017b) were synthesized, and the NPs used by the present study and by Hansein et al. (Hassanein et al., 2019) were obtained commercially. The size of NP is extremely important for the process since it can affect the binding and activation of membrane receptors and the expression of proteins (Jiang et al., 2008), thus acting to stimulate the growth of methanogenic archaea (Mu et al., 2011b).

For better visualization, a cut in the graph was made of particles found only in nano size, which are shown in Figure 1b. The average size of these Fe_3O_4 NP was 23.56 ± 0.05 nm, which can be considered a greater size since some authors have reported a decrease in CH_4 production by using Fe NPs greater than 55 nm (Gonzalez-estrella et al., 2013; Hassanein et al., 2019). Another important factor is that these Fe_3O_4 NPs used in this work have a spherical shape (Figure 2), and this has improved the production of CH_4 in the work of Abdsalam et al. (Abdelsalam et al., 2017b) which is explained by the greater membrane wrapping time required for the elongated particles.

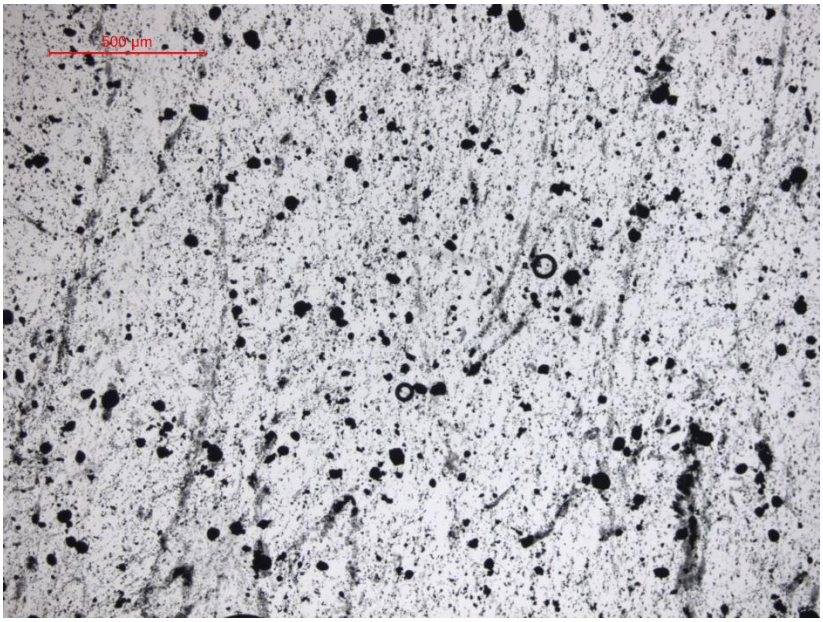

Figure 2- Mastersize images (50x) showing Fe_3O_4 NP

However, it is worth mentioning that besides size, another important factor to stimulate CH_4 production is the concentration in which the NP, in addition to the type of substrate being used and the interaction between them (Abdelsalam et al., 2016). For this reason, preliminary tests of BMP with different concentrations of NP Fe_3O_4 were carried out within the co-digestion of residues. It is worth mentioning that a zeta potential (ZP) analysis was carried out for the nanoparticles, to evaluate their dispersibility in the medium. However, it was not possible to obtain results, because they are magnetic particles, and have sizes larger than nano, the dispersion remained unstable, as has already been reported by Gonzalez et al. (Gonzalez-estrella et al., 2013).

3.2 Bacth preliminary assays

Table 4 shows the results of the accumulated CH_4 in triplicate of each of the tests with different concentrations of Fe_3O_4 NP, and Figure 3 shows the graph of CH_4 accumulated obtained over time.

Table 4. Final cumulative CH_4 production of co-digestion in different concentration of Fe_3O_4 NP

Assay	Cumulative CH_4 ($NmLVS^{-1}$)[a]
Control	123.24 ± 9.60
NP 1	116.49 ± 17.45
NP 2	140.13 ± 95.60
NP 3	117.90 ± 10.68
NP 4	133.02 ± 106.29

[a]: mean of three replicates ± standard variation

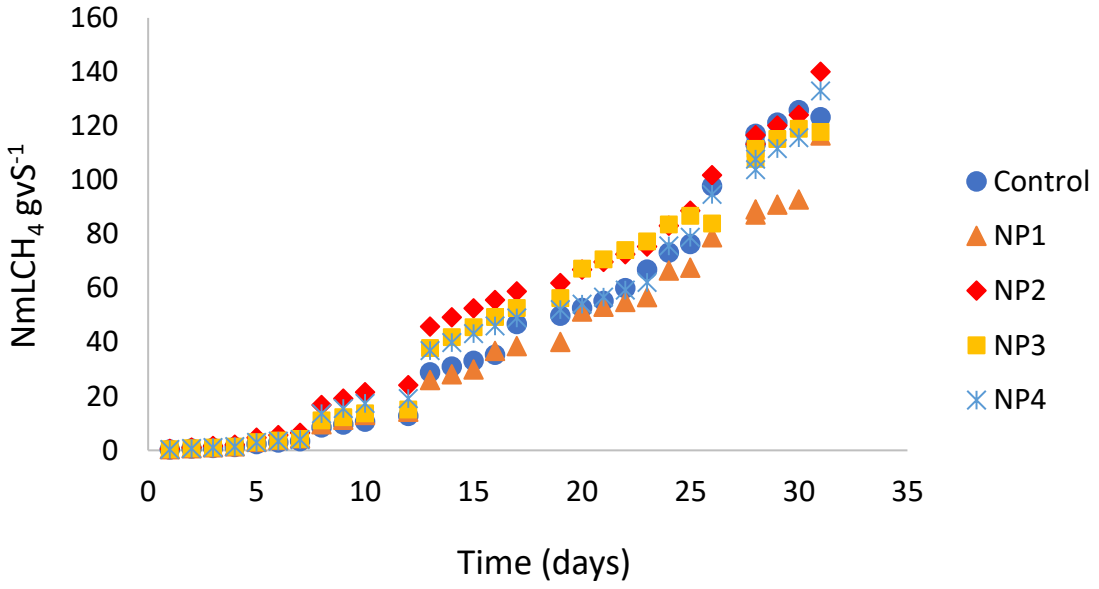

Figure 3. Cumulative CH_4 production testing four concentrations of Fe_3O_4 nanoparticle (NP) additions to co-digestion. NP1: 1 mg L^{-1}; NP2: 5 mg L^{-1}; NP3: 10 mg L^{-1}; NP4: 20 mg L^{-1}

Analysis of variance (ANOVA) was performed between the tests, but there was no significant difference between treatments with different concentrations of Fe_3O_4 NP (p-value = 0.1357 with $p < 0.05$). Although there is no significant difference, it can be seen that the NP 2, NP 3 and NP 4 assays obtained CH_4 production greater than the control (Figure 3) and the NP 1 was below the control. Table 4 shows that the NP 2 test showed a 13% increase in CH_4 production compared to the control, while the NP 4 test showed a 7% increase in CH4 production.

In the work of Hansein et al. (Hassanein et al., 2019), they obtained a 25% increase in CH_4 production, using 15 mg L^{-1} of NP Fe_3O_4 in BMP assays, with poultry litter residues, under mesophilic conditions. However, in this same work, a higher concentration of CH_4 (34%) was obtained using NP Ni with a concentration of 12 mg L^{-1}. The difference in substrates, experimental conditions, and the origin of the inoculum can influence these differences in production. It is worth mentioning the short lag phase

found in the experiment could be because of the addition of Fe_3O_4 NPs, according to Krongthamchat et al. (Krongthamchat et al., 2006).

Even in the preliminary test no significant difference in CH_4 production was observed, in the s-CSTR reactor, the concentration of 5 mg L^{-1} of NP Fe_3O_4 was used, the condition of the NP 2 experiment, which showed a greater increase in the CH_4 production concerning the control. It is also known that nanoparticles are not easy to be separated from biodegradable wastes, which may subsequently cause accumulation of inorganic pollutants (usually heavy metals) inside anaerobic digesters (Zhu et al., 2021). For this reason, it was decided to choose a lower concentration of NPs, to cause a less environmental impact on AD. With this, it is possible to observe differences in the operation of the continuous reactor with the addition of NP compared to the same reactor operation, but without the addition of NP (Volpi et al., 2021b).

3.3 Semi-Continuous Stirred Tank Reactor performance

3.3.1 Biogas production and reactor efficiency

Figure 4 shows the results obtained from CH_4 production and removal of organic matter throughout the different OLRs used. In phases I and II, it is possible to observe an intense variation in the removal of organic matter, varying between approximately 30% and 70%. Along with this, there was also a small variation in CH_4 production, ranging from 0.1 to 0.5 $NLCH_4$ gVS^{-1}. These variations are characteristic of the acidogenic phase, marking the start-up of the reactor. After approximately 60 days, that is, phase III, both the production of CH_4 and the removal of organic matter maintain greater stability, indicating the possibility that the reactor is entering the methanogenic phase. Between phase IV and phase V it is possible to observe that the production of CH_4 remains around

0.5 and 1 $NLCH_4$ gVS^{-1} showing a trend in the increase of CH_4 production. In phase VI, after the addition of Fe_3O_4NP, there was a 40% increase in CH_4 production (122 days), obtaining the highest CH_4 production throughout the entire operation, with 2.8 ± 0.1 $NLCH_4$ gVS^{-1} and removal of 71 ± 0.9% of organic matter. In phase VII, the production of CH_4 begins to show a decrease, but the removal of the organic matter remains stable. In phase VII, the production of CH_4 remains low (0.09 ± 0.03 $NLCH_4$ gVS^{-1}) and the removal of organic matter continues to decrease (51 ± 2.8%), reaching the collapse of the reactor in phase IX.

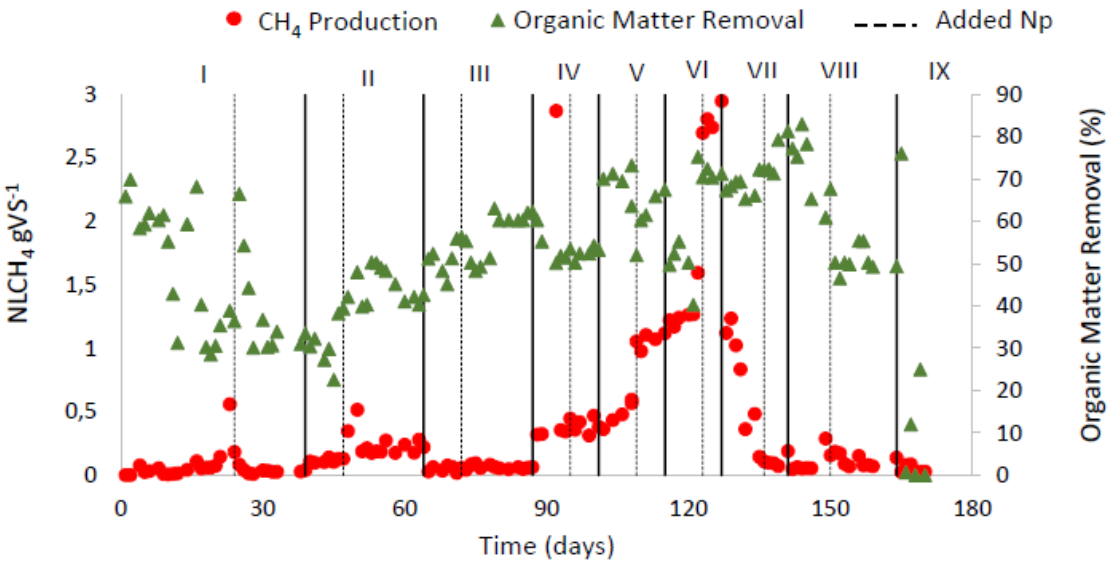

Figure 4. Methane production and organic matter removal along with the reactor operation according to the applied OLRs (g VS L^{-1} day^{-1}): 2.0 (Phase I); 2.35 (Phase II); 3.0 (Phase III); 4.0 (Phase IV); 4.7 (Phase V); 5.5 (Phase VI); 6.6 (Phase VII); 8.0 (Phase VIII); 9.0 (Phase IX)

In our previous study Volpi et al., 2021b (the operation was carried out in a reactor with co-digestion of the same residues as in this work and under the same experimental conditions) was obtained 0.233 ± 1.83 $NLCH_4$ gSV^{-1} and 83.08 ± 13.30% organic matter removal. The present work had an increase of 91% of the production of CH_4 about the

previous work. This fact confirms that the presence of Fe_3O_4 NP contributed to better development and performance of the microbial community in the consumption of organic matter and conversion to CH_4 since Fe is a growth stimulant of methanogenic *Archaeas* and they are dependent on this element to enzyme synthesis (Choong et al., 2016; Ni et al., 2013). In addition, the maximum production of CH_4 from the work of Volpi et al., 2021b was in the OLR of 4.16 gVS L^{-1} day^{-1}, with the reactor collapsed in the OLR of 5.23 gVS L^{-1} day^{-1}. In the present work it was possible to obtain the maximum performance of the reactor in the OLR of 5.5 gVS L^{-1} day^{-1}, and collapsing with OLR 9 gVS L^{-1} day^{-1}, showing that the presence of Fe_3O_4NP made it possible to work with larger OLRs, resulting in greater volumes of feed in the reactor and consequent treatment higher volume of waste.

In the work of Hassanein et al. (Hassanein et al., 2019) using poultry litter for BMP assays, with the addition of 15 mg L^{-1} Fe_3O_4 NP, maximum cumulative production of 339 $mLCH_4$ gVS^{-1} was obtained. In the work of Abdsalam et al. (Abdelsalam et al., 2017b) in BMP tests with manure, 20 mg L^{-1} of Fe_3O_4 NP was added and 351 $mLCH_4$ gVS^{-1} was obtained. The literature has reported the use of NP in BMP assays, and smaller vials to assess NP activity. In the present study, it was possible to obtain 85% more CH_4 than those reported in the literature. It is worth mentioning that the use of the substrate with the type of NP interferes with the production of CH_4, in addition to the concentration of NP has been used also interfere. In the work by Abdsalam et al. (Abdelsalam et al., 2016) and Uemura (Sh, 2010), it was confirmed that the use of Ni NP was the one that best impacted the increase in CH_4 production in the use of municipal solid waste. In the study by Ali et al. (Ali et al., 2017) four concentrations of Fe_3O_4 NPs (50, 75, 100, and 125 mg L^{-1}) were tested in assays with municipal solid waste. The results showed that the

addition of 75 mg L^{-1} Fe_3O_4NPs increases the CH_4 production by 53.3%. In contrast, less CH_4 production was observed by adding a high concentration of Fe_3O_4 NPs.

Absalam et al. (Abdelsalam et al., 2016) showed that the addition of Fe_3O_4 magnetic NPs increased bacterial activity during onset up to 40 days of HRT. However, in the present study, an increase in bacterial activity was observed in the middle of the operation (phase IV, V, and VI, after 90 days), in agreement with Quing Ni et al (Ni et al., 2013) who indicated that during the exposure of 50 mg L^{-1} of magnetic NPs the adverse effects were insignificant in bacteria and concluded that magnetic NPs appeared to be non-toxic during long-term contact. The best performance is due to the presence of $Fe2^{+}$ / $Fe3^{+}$ ions, introduced into the reactor in the form of nanoparticles that could be adsorbed as the growth element of anaerobic microorganisms (Abdelsalam et al., 2016). In addition, Fe_3O_4 magnetic NP ensures a distribution of the iron ions in the slurry through the corrosion of the NPs, thus maintaining the iron requirement of the reactor supplied (Abdelsalam et al., 2016). The presence of NPs also shows a possible effect on the hydrolysis-acidification process, increasing the reduction of the substrate, since there were increasing amounts of organic matter removed in phases V, VI and VII, and a subsequent increase in the production of CH_4.

3.3.2 pH, ORP, and Alkalinity indications

Figure 5a shows the results obtained from the reactor inlet and outlet pH, as well as the results of oxide-reduction potential (ORP).

It is possible to observe that in the first days, the exit pH is very acid, around 6 and the ORP values vary a lot. In addition, the pH in was daily adjusted to a neutral pH. These characteristics mark acidogenesis, and the intense oxidation-reduction reactions typical of the AD process (Vongvichiankul et al., 2017). After 60 days, it is possible to

observe that the pH remains between 7.5 and 8 until the end of the operation, indicating that from this date on, the reactor entered the methanogenesis phase, maintaining the pH stable and no more adjustment of the pH at the entrance. The same is true for ORP values, which after 60 days, remain around -460 and -490 mV.

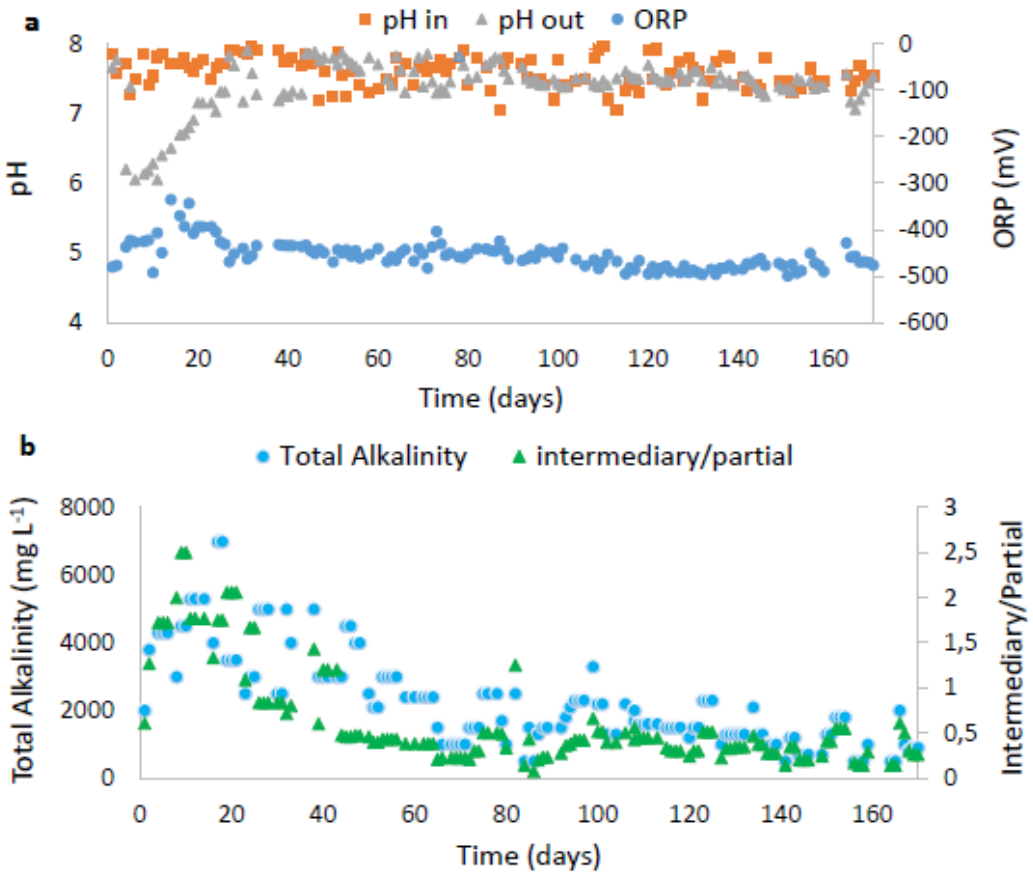

Figure 5. pH, Oxidation Reduction Potential (a) and Alkalinity (b) along with the reactor operation according to the applied OLRs (g VS L^{-1} day^{-1}): 2.0 (Phase I); 2.35 (Phase II); 3.0 (Phase III); 4.0 (Phase IV); 4.7 (Phase V); 5.5 (Phase VI); 6.6 (Phase VII); 8.0 (Phase VIII); 9.0 (Phase IX)

In our previous work, methanogenesis was established only after 90 days, with stabilization of the pH and ORP values (Volpi et al., 2021b). In this present work, methanogenesis was established before, next 60 days, and everything indicates that it may

have been due to the presence of NPs, since Abdsalam et al. (Abdelsalam et al., 2017b) showed that the addition of Fe_3O_4 NP reduces the lag phase of AD. In addition, Feng et al. (Feng et al., 2014) showed that the addition of Fe in the AD system can directly serve as an electron donor to reduce CO_2 in CH_4 through autotrophic methanogenesis causing improvement of CH_4 production, according to the reactions below (1), (2) and (3).

$$4H_2 + Fe_3O_4 = 4H_2O + 3Fe^0 \quad (1)$$

$$CO_2 + 4Fe^0 + 8H^+ = CH_4 + 4Fe^{2+} + 2H_2O \quad (2)$$

$$CO_2 + 4H_2 = CH_4 + 2H_2O \quad (3)$$

From this process the substrates would be deprived of hydrogen ions (H^+) which will increase the pH of the substrate and the capture of CO_2 also prevents the formation of carbonic acid, increasing the pH of the substrate (Abdelsalam et al., 2017b). This may explain the increase in pH after 24 days (Table 3) since it was the first addition of Fe_3O_4 NPs. The methanogenesis process stage was also stimulated, as this nano additive served as an electron donor that could reduce CO_2 to CH_4.

At the beginning of the operation, the ORP varied between -350 and -550 mV, and this variation is a characteristic of acidogenesis and reactor start-up (Volpi et al., 2021b). However, this variation in a start-up was much smaller than reported in Volpi et al. (2021b) (-800 and -300 mV) indicating greater stability of the operation. After approximately 40 days (Figure 5a), it is observed that the ORP remains practically constant until the end of the operation, varying between -480 and -400 mV, although the literature shows that the ORPs characteristic of the acidogenic and methanogenic phase is between -330 and -428 mV (Golkowska and Greger, 2013). This demonstrates the stability of the prevalence targeting of metabolic routes for the production of CH_4 and development of methanogenic A*rchaeas* entire operation, which may have been

optimized by the presence of Fe_3O_4 NP, since in the work of the same reactor operated and without the NPs the ORP values in methanogenic phase varied much more (-650 and -400 mV). These low ORP values in the system are characteristic of the presence of Fe NPs since they reduce the system's ORP to increase the conversion of complex compounds to volatile fatty acids and to be able to provide ferrous ions for the growth of fermentative and methanogenic *Archeae* (Lee and Lee, 2019).

It is important to demonstrate that the ORP values practically constant are in agreement with the OA values (section 3.3.3), which are in extremely low concentrations when the reactor stabilizes in methanogenesis. Here it is worth emphasizing the differences in the ORP values found in the literature are varied due to the different raw materials applied, experimental conditions and the type of NP used.

Figure 5b shows the results of alkalinity obtained during the operation. It is possible to observe that the alkalinity is high up to 60 days, being following the pH and ORP and also with the presence of OA (Figure 6a section 3.3.3) characterizing the acidogenic step of the process. After 60 days, the intermediate/partial alkalinity (IA/PA) is below 0.3, which is considered ideal for AD, as it demonstrates stability (Ripley et al., 1986). As was the behavior of the ORP, the IA/PA also remained stable throughout the process, showing self-regulation of methanogenesis. In our previous study (Volpi et al., 2021b), this stability of alkalinity also only happened after 90 days, confirming the hypothesis that the presence of Fe_3O_4NP has reduced the lag phase. In addition, Fe3O4NP can absorb inhibitory compounds and act as a pH buffer, further improving the alkalinity of the process.

3.3.3 Degradation routes: OA, Carbohydrate, and Alcohol indications

Figure 6 shows the results obtained from OA and carbohydrates and alcohols.

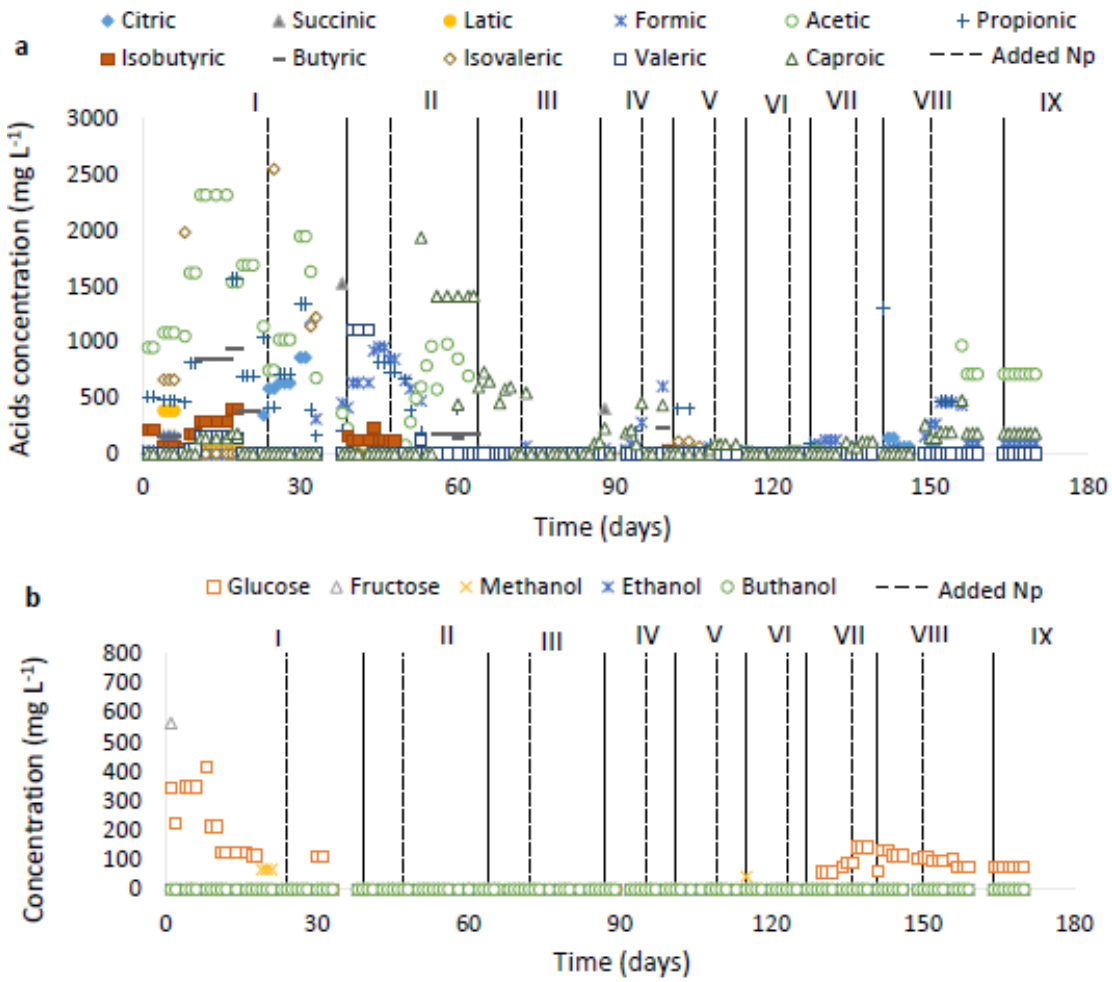

Figure 6. Values of Organic acids (a), Carbohydrates, and Alcohols (b) along with the reactor operation according to the applied OLRs (g VS L^{-1} day^{-1}): 2.0 (Phase I); 2.35 (Phase II); 3.0 (Phase III); 4.0 (Phase IV); 4.7 (Phase V); 5.5 (Phase VI); 6.6 (Phase VII); 8.0 (Phase VIII); 9.0 (Phase IX)

In phases, I and II (Figure 6a) the presence of high concentrations of OA confirms the start-up of the reactor, in the acidogenic phase. After 60 days, the concentrations of these OA decrease considerably, indicating the entrance of the reactor in the

methanogenic phase and agreeing with what was discussed in the previous sections (section 3.3.1, 3.3.2).

At the beginning of the reactor operation (phase I), the concentration of acetic acid is relatively high, which is favorable for the CH_4 production process, since it is the main precursor of the CH_4 metabolic route (Wiegant et al., 1986). In addition to acetic acid, there is also the presence of propionic acid, which in concentrations above 1500 mg L^{-1} can be inhibitory to the metabolic pathway of CH_4 production (Wang et al., 2009). But, this concentration decrease in phase I and phase II, and in acetic acid concentration increase at the end of phase II, indicating that the route of conversion of propionic acid to acetic acid may have prevailed at the beginning of the operation, as also occurred in our previous study (Volpi et al., 2021b). It is worth mentioning that in the presence of low H_2 pressure, propionic acid consumption is favored (Wiegant et al., 1986), and Fe is a trace element whose main substrate for oxidation-reduction reactions is H_2 (Choong et al., 2016). The presence of Fe_3O_4 NP may have favored the consumption of H_2, according to reaction 4 and reaction 1, and consequently helped in the consumption of propionic acid, favoring the formation of acetic acid and this having been converted to CH_4.

$$H_2 \leftrightarrow 2e^- + 2H^+ \quad (4)$$

In phases I and II it is also possible to observe the presence of formic acid, and its conversion to acetic acid is typical of acidogenesis (Choong et al., 2016). Therefore, in addition to the conversion of propionic acid to acetic acid, the conversion of formic acid to acetic acid may also have occurred at the end of acidogenesis, marking the beginning of methanogenesis (phase III-Figure 6a). In addition, the presence of Fe NP can increase the production of acetate and donate electrons for direct conversion of CO_2 into CH_4 by autotrophic via methanogenesis (Feng et al., 2014).

The Fe (III) reduction reaction is a favorable process to directly oxidize organics into simple compounds (Romero-Güiza et al., 2016), increasing the consumption of OA, and eliminate compounds that may be toxic to the process, by stimulating microbial growth, synthesis of necessary enzymes within the oxidation-reduction reactions and consequently greater efficiency in the digestion of organic matter (Choong et al., 2016; Lee and Lee, 2019). The positive effect of Fe (III) supplementation was attributed to the favorable redox conditions, which all evited the thermodynamic limitations on organic acid degradation. Furthermore, Fe (III) can precipitate H_2S minimizing related inhibition phenomena (Romero-Güiza et al., 2016). The control of OA can allow a greater capacity of feed of the digester, without affecting the performance of digestion significantly (Zhang et al., 2015), this is what happened in the present study, since the used OLRs were higher than the experiment previous (Volpi et al., 2021b), with higher volumes of feed, and a stable operation, reaching high CH_4 production.

The presence of caproic acid draws attention at the end of phase II and the beginning of phase III (Figure 6a). Caproic acid is produced by lengthening the chain of short-chain volatile fatty acids, such as acetic acid and butyric acid through an oxidation reaction, in which some species can gain energy by increasing the length of the volatile organic acids chain with reducing substrates such as ethanol and lactic acid (Owusu-Agyeman et al., 2020). However, in the operation, neither the presence of lactic acid nor ethanol was detected (Figure 6a and Figure 6b), but it seems that Fe_3O_4NP may have acted as this reducing substrate, gaining electrons and allowing an increase in the chain of butyric and acetic acids. This fact may also have been caused by the continuous feeding process of the reactor, in which Fe_3O_4NP was added with a certain frequency, having a constant availability of the electron donor for the formation of caproic acid and in agreement with what was reported by Owusu-Agyeman et al. (Owusu-Agyeman et al.,

2020). Even with the possible change of the route for the production of caproic acid, the production of CH_4 prevailed, indicating the self-regulation of the microbial consortium for the metabolic route of CH_4. Although not the focus of this work, the addition of Fe_3O_4 NP with the residues of the sugarcane industry can stimulate the production of caproic acid, and organic acid has high added value because it is used as antimicrobials for animal feed and precursors aviation fuel (Angenent et al., 2016).

Figure 6b shows that at the beginning of the operation there was greater availability of glucose, and when the reactor entered the phase of methanogenesis, the concentration of this glucose was very low, indicating the self-regulation of the process for CH_4 production. When the reactor begins to decrease its production of CH_4, phases VII and VIII, the concentration of glucose increases again, indicating the start of the collapse of the operation.

2.6 Microbial community characterization

Figure 7 shows the observed values of richness (number of species-a), and the calculated values from diversity (Shannon index-b) and wealth estimate (Chao1 estimator-c) of the Samples. The results show that the number of species (Figure 7a) and richness (Figure 7b) of the A1 samples was higher than that of the A2 sample. This behavior is as expected for these results since the A1 samples are samples from the initial inoculum, that is, from the inoculum without having been inserted into the reactor. The A2 samples are from the inoculum when the CH_4 production was stabilized, that is to say, that the microbial community present is already "selected" for the specific metabolic route of CH_4 production according to the substrates used. In addition, the inoculum of Sample A1 comes from a mesophilic reactor, while Sample A2 comes from a thermophilic reactor. Process temperature differences may also have led to this difference between

species of microorganisms. These results are consistent with what happened in our previous work (Volpi et al., 2021b) indicating that the presence of NP did not influence the diversity of microorganisms and the change in the microbial community from one sample to another.

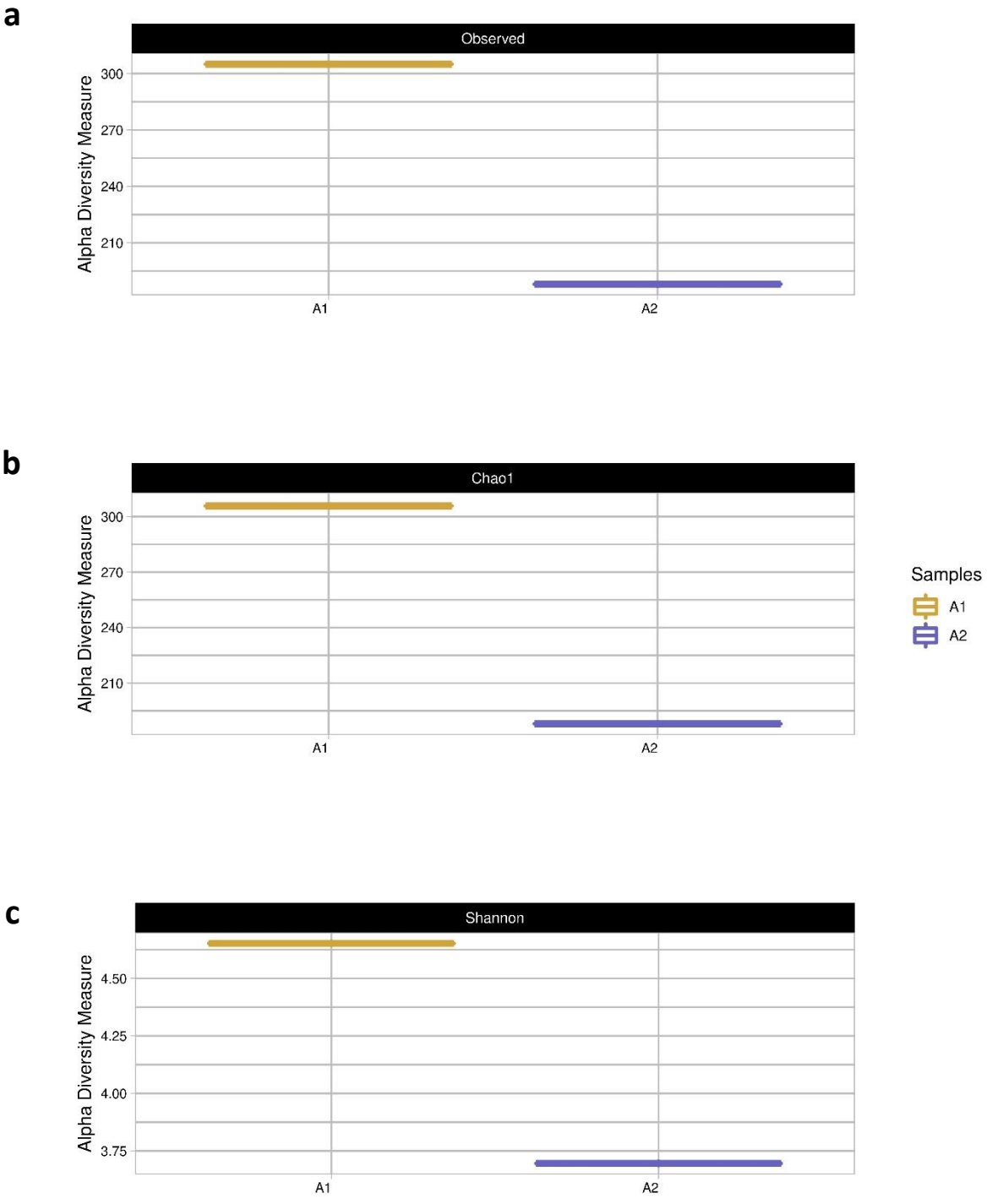

Figure 7. Observed values of (A) richness (number of species), (B) richness estimate (Chao1 estimator), and (C) calculated values of diversity (Shannon index) of Sample 1 (seed sludge) and Sample 2 (sludge from the s-CSTR stable operation, Phase IV)

The Shannon index obtained from sample A1 was close to 5.0, while that from sample A2 was less than 3.75. As discussed in Volpi et al., 2021b, when the value of the Shannon index is greater than 5.0, it indicates greater microbial diversity in anaerobic digesters (de Souza Moraes et al., 2019). Thus, it can be seen that the A2 sample has a much lower microbial diversity than the A1, since these microorganisms are in stabilized metabolic routes for CH_4 production, indicating that this microbial community is even more specific.

Figure 8 shows the results obtained from phylum in relation to *Bacteria* order (a) and *Archaea* order (b) from samples A1 and A2.

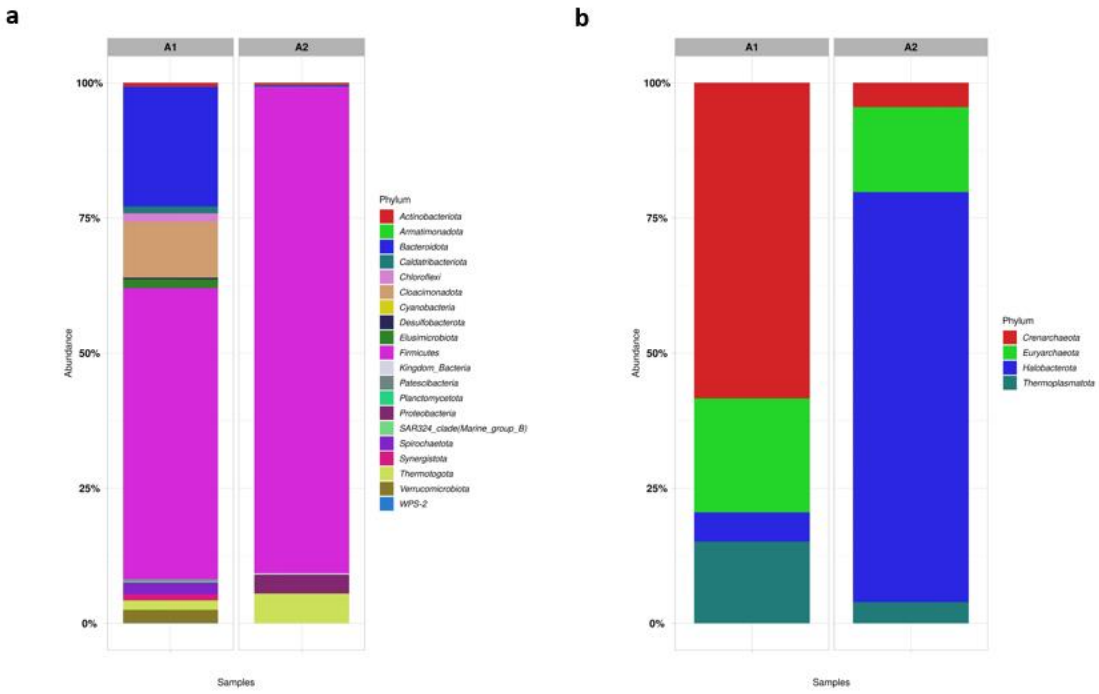

Figure.8 Relative abundance of microorganisms at the phylum level from *Bacteria* order (a) and *Archaea* order (b) from the seed sludge- Sample A1 and from the s-CSTR sludge with stable CH_4 production-Sample A2.

Following what was discussed above, the phyla variety found in sample A1 (Figure 8a) is much larger than those found in A2. In sample A1 the principals phyla found from *Bacteria* order was: (~25%) *Bacteroidota*, (~15%) *Cloacimonadota*, (~50%) *Firmicutes* and (~2%) *Spirochaetota*. Microorganisms of the phylum *Bacteroidota*, *Cloacimonadota*, and *Spirochaetota* are generally found in mesophilic processes and are bacteria responsible for the fermentative and hydrolytic steps of AD (Xie et al., 2020; Zhang et al., 2021). The presence of these three phyla in the A1 sample and the absence of them in the A2 sample indicates how temperature influenced the change in the bacterial community since the A1 inoculum comes from a mesophilic process. The large presence of the *Firmicutes* phylum is to be expected since they are one of the main phyla of anaerobic processes, and most cellulolytic bacteria belong to them (Wu et al., 2020). In sample A2 the main phyla found are (~80%) *Firmicutes*, (~2%) *Protobacteria*, and (~5%) *Thermotogota*. The *Thermotogota* phylum is characteristic of thermophilic processes (Wang et al., 2018), and bacteria of the *Protobacteria* phylum are characteristic for degrading lignocellulosic material (Wu et al., 2020). It is important to mention that these two last phyla are present in smaller proportions in sample A1, indicating the possibility of a change in the microbial community due to experimental conditions and used substrates. Furthermore, in the previous co-digestion work (Volpi et al., 2021b) these same phyla were found in the sample when the reactor was stabilized for CH_4 production, indicating that the presence of Fe_3O_4 NP did not influence the change in the microbial community concerning order Bacteria. Zhang et al. (Zhang et al., 2021)showed that the

presence of *Proteobacteria* followed by *Firmicutes* the bacteria were the central syntrophic acetogenins for propionate oxidation via the methylmalonyl-CoA pathway, perhaps indicating the presence of this metabolic route when CH_4 production stabilized, as discussed in section 3.3.3.

About *Archaea* order phyla, in sample A1 it was observed (~25%) *Euryarchaeota* and in sample A2 (~20%) of the same phylum. This phylum is characteristic of methanogenic *Archaeas*, responsible for the production of CH_4. In addition to this main phylum, other phyla of the *Archaea* order were also found, such as *Crenarchaeota*, *Halobacterota*, but they are not highly relevant for the results of CH_4 production, which is the focus of this work.

Figure 9 shows the main genera found for samples A1 and A2 to the order *Bacteria* (a) and the order *Archaea* (b). As previously discussed, the A1 sample presented a very large microbial diversity, with no genus that was predominant in the process about the *Bacteria* order. Its genera of microorganisms come from the main phyla (*Bacteroidota*, *Cloacimonadota*, *Firmicutes*) and are characteristic of acidogenic and hydrolytic processes.

Sample A2 has some genera of the order *Bacteria* that stand out, such as (~5%) *Defluvitoga*, (~3%) *Hydrogenispora*, (~9%) *Ruminiclostridium*. These genera were also present in the reactor operation without the presence of Fe_3O_4 NP (Volpi et al., 2021b).

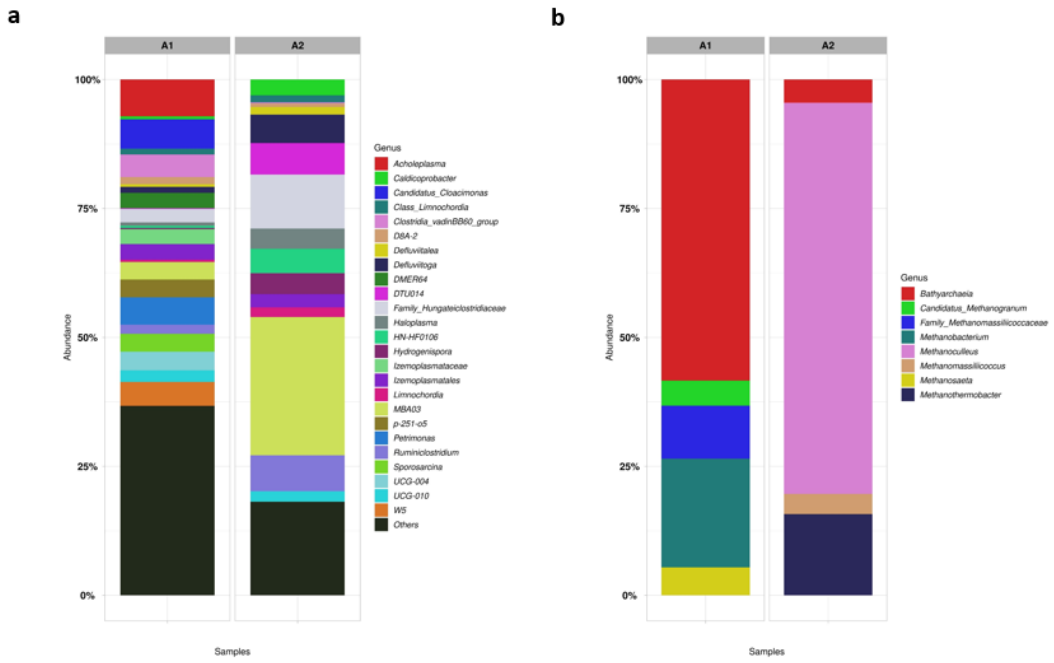

Figure 9. Relative abundance of microorganisms at the genus level from *Bacteria* order (a) and *Archaea* order (b) from the seed sludge- Sample A1 and from the s-CSTR sludge with stable CH_4 production-Sample A2.

Defluvitoga genus, belonging to the phylum *Thermotogota*, is reported to be dominant in the degradation of organic materials in CSTRs or thermophilic bioelectrochemical reactors (Guo et al., 2014). *Ruminiclostridium*, belonging to the phylum *Firmicutes*, are hydrolytic bacteria characterized by metabolizing cellulosic materials, with a high concentration of lignocellulose (Peng et al., 2014), which is the case of residues used in reactor operation. In the work by Kang et al. (Kang et al., 2021) wheat straw was used for anaerobic digestion, and bacteria belonging to the genus *Ruminiclostrium* and *Hydrogenispora* were found as the main microorganisms. This fact leads to the association that such bacteria are present in the degradation of lignocellulose substrates since wheat straw and residues from the present work have a similar composition.

Hydrogenispora is acetogenic bacteria, which can ferment carbohydrates such as glucose, maltose, and fructose into acetate, ethanol, and H_2 (Kang et al., 2021). These bacteria can act in conjunction with hydrogenotrophic methanogens. In Figure 9b, the predominant methanogenic *Archaea* in sample A2 was (~70%) *Methanoculleus*. This methanogenic *Archaea* is characterized by acting syntrophic oxidation of acetate (SAO) coupled with hydrogenotrophic methanogenesis (Schnürer et al., 1999). Furthermore, it was also the main methanogenic found in the work by Volpi et al. (2021b). Therefore, it can be seen that despite the addition of NP in the reactor, the presence of the microbial community was not altered and therefore, the metabolic routes were also the same. The presence of NPs only encouraged the activity of the methanogenic *Archaea*, but since the substrates used and experimental conditions were the same, there was no change in the metabolic route. The genus (~15%) *Methanotermobacter* was also found in sample A2. This genus is characterized by being present in thermophilic anaerobic digestions and belongs to the obligate-hydrogenotrophic methanogens (Li et al., 2020). This fact corroborates the possibility that the predominant metabolic route in the co-digestion of vinasse, filter cake, and deacetylation liquor is acetate (SAO) coupled with hydrogenotrophic methanogenesis. Furthermore, it was discussed in section 3.3.3 that in the presence of low H_2 pressure, propionic acid consumption is favored, and Fe is a trace element whose main substrate for oxidation-reduction reactions is H_2. This confirms the fact that the presence of Fe_3O_4 NP may have reinforced that the main metabolic pathway for the co-digestion of these residues is through hydrogenotrophic methanogens.

In sample, A1 (Figure 9a) were found (~20%) *Methanobacterium* and (~7%) *Methanosaeta. Methanobacterium* is known as hydrogenotrophic methanogens while *Methanosaeta* is known as obligate-acetoclastic methanogen and has a strong affinity to acetate (Li et al., 2020). These two genera are not found in sample A2, indicating how

there was a change in the microbial community from sample A1 to A2 due to different substrates and experimental conditions.

4. CONCLUSIONS

Through the present work, it is possible to conclude that the use of Fe_3O_4 NP is an additive that optimized the co-digestion of 1G2G ethanol industry residues, providing an increase of approximately 90% in CH_4 production. Despite not having significant differences between the different concentrations of NP in the batch process, the concentration of 5 mg L^{-1} of Fe_3O_4 NP was ideal for a stable continuous operation, with production stimulation, and without process inhibitions.

These nanoparticles proved to favor the reduction of the lag phase of the process, through a stabilized reactor operation. The reactor collapsed in OLRs of 9 gVS L^{-1} day^{-1}, being an ORL almost 2 times larger than that used in the operation without the presence of NP (9 *vs* 5 gVS L^{-1} day^{-1}). Furthermore, the methanogenesis was stabilized after 60 days of operation, being 30 days earlier than the operation without the addition of NP.

Fe_3O_4 NP did not influence the possible metabolic pathways of the process, on the contrary, they stimulated the growth of methanogenic *Archaea*, reinforcing that the main metabolic pathway of these residues in co-digestion is through hydrogenotrophic methanogenesis. *Methanoculleus* are the main methanogenic *Archea* found in the process, and *Defluvitoga*, *Ruminiclostridium*, and *Hydrogenispora* are the main genus of *Bacteria* order in process, both with or without the addition of NP.

5. REFERENCES

Abdelsalam, E., Samer, M., Attia, Y.A., Abdel-Hadi, M.A., Hassan, H.E., Badr, Y.,

2017a. Effects of Co and Ni nanoparticles on biogas and methane production from anaerobic digestion of slurry. Energy Convers. Manag. 141, 108–119. https://doi.org/10.1016/j.enconman.2016.05.051

Abdelsalam, E., Samer, M., Attia, Y.A., Abdel-Hadi, M.A., Hassan, H.E., Badr, Y., 2017b. Influence of zero valent iron nanoparticles and magnetic iron oxide nanoparticles on biogas and methane production from anaerobic digestion of manure. Energy 120, 842–853. https://doi.org/10.1016/j.energy.2016.11.137

Abdelsalam, E., Samer, M., Attia, Y.A., Abdel-Hadi, M.A., Hassan, H.E., Badr, Y., 2016. Comparison of nanoparticles effects on biogas and methane production from anaerobic digestion of cattle dung slurry. Renew. Energy 87, 592–598. https://doi.org/10.1016/j.renene.2015.10.053

Ali, A., Mahar, R.B., Soomro, R.A., Sherazi, S.T.H., 2017. Fe3O4 nanoparticles facilitated anaerobic digestion of organic fraction of municipal solid waste for enhancement of methane production. Energy Sources, Part A Recover. Util. Environ. Eff. 39, 1815–1822. https://doi.org/10.1080/15567036.2017.1384866

Angenent, L.T., Richter, H., Buckel, W., Spirito, C.M., Steinbusch, K.J.J., Plugge, C.M., Strik, D.P.B.T.B., Grootscholten, T.I.M., Buisman, C.J.N., Hamelers, H.V.M., 2016. Chain Elongation with Reactor Microbiomes: Open-Culture Biotechnology to Produce Biochemicals. Environ. Sci. Technol. 50, 2796–2810. https://doi.org/10.1021/acs.est.5b04847

APHA, AWWA, W., 2012. Standard Methods for the Examination of Water and Wastewater, twenty-sec. ed. Washington, DC.

Brenelli, L.B., Figueiredo, F.L., Damasio, A., Franco, T.T., Rabelo, S.C., 2020. An integrated approach to obtain xylo-oligosaccharides from sugarcane straw: from lab to pilot scale. Bioresour. Technol. 123637.

https://doi.org/10.1016/j.biortech.2020.123637

Choong, Y.Y., Norli, I., Abdullah, A.Z., Yhaya, M.F., 2016. Impacts of trace element supplementation on the performance of anaerobic digestion process: A critical review. Bioresour. Technol. 209, 369–379. https://doi.org/10.1016/j.biortech.2016.03.028

de Souza Moraes, B., Mary dos Santos, G., Palladino Delforno, T., Tadeu Fuess, L., José da Silva, A., 2019. Enriched microbial consortia for dark fermentation of sugarcane vinasse towards value-added short-chain organic acids and alcohol production. J. Biosci. Bioeng. 127, 594–601. https://doi.org/10.1016/j.jbiosc.2018.10.008

Demirel, B., Scherer, P., 2011. Trace element requirements of agricultural biogas digesters during biological conversion of renewable biomass to methane. Biomass and Bioenergy 35, 992–998. https://doi.org/10.1016/j.biombioe.2010.12.022

Demirel, B., Scherer, P., 2008. The roles of acetotrophic and hydrogenotrophic methanogens during anaerobic conversion of biomass to methane: A review. Rev. Environ. Sci. Biotechnol. 7, 173–190. https://doi.org/10.1007/s11157-008-9131-1

Deublin, D., Steinhauser, A., 2008. Biogas from Waste and Renewable Resources: An Introduction. Wily Online Library, Weinheim, Germany. https://doi.org/1010029783527621705

Djalma Nunes Ferraz Júnior, A., Koyama, M.H., de Araújo Júnior, M.M., Zaiat, M., 2016. Thermophilic anaerobic digestion of raw sugarcane vinasse. Renew. Energy. https://doi.org/10.1016/j.renene.2015.11.064

Feng, Y., Zhang, Y., Quan, X., Chen, S., 2014. Enhanced anaerobic digestion of waste activated sludge digestion by the addition of zero valent iron. Water Res. 52, 242–250. https://doi.org/10.1016/j.watres.2013.10.072

Fuess, L.T., Kiyuna, L.S.M., Ferraz, A.D.N., Persinoti, G.F., Squina, F.M., Garcia, M.L., Zaiat, M., 2017. Thermophilic two-phase anaerobic digestion using an innovative fixed-bed reactor for enhanced organic matter removal and bioenergy recovery from sugarcane vinasse. Appl. Energy 189, 480–491. https://doi.org/10.1016/j.apenergy.2016.12.071

Golkowska, K., Greger, M., 2013. Anaerobic digestion of maize and cellulose under thermophilic and mesophilic conditions – A comparative study. Biomass and Bioenergy 56, 545–554. https://doi.org/https://doi.org/10.1016/j.biombioe.2013.05.029

Gonzalez-estrella, J., Sierra-alvarez, R., Field, J.A., 2013. Toxicity assessment of inorganic nanoparticles to acetoclastic and hydrogenotrophic methanogenic activity in anaerobic granular sludge. J. Hazard. Mater. 260, 278–285. https://doi.org/10.1016/j.jhazmat.2013.05.029

Guo, X., Wang, C., Sun, F., Zhu, W., Wu, W., 2014. A comparison of microbial characteristics between the thermophilic and mesophilic anaerobic digesters exposed to elevated food waste loadings. Bioresour. Technol. 152, 420–428. https://doi.org/10.1016/j.biortech.2013.11.012

Hagos, K., Zong, J., Li, D., Liu, C., Lu, X., 2017. Anaerobic co-digestion process for biogas production: Progress, challenges and perspectives. Renew. Sustain. Energy Rev. 76, 1485–1496. https://doi.org/10.1016/j.rser.2016.11.184

Hassanein, A., Lansing, S., Tikekar, R., 2019. Bioresource Technology Impact of metal nanoparticles on biogas production from poultry litter. Bioresour. Technol. 275, 200–206. https://doi.org/10.1016/j.biortech.2018.12.048

Janke, L., Leite, A., Batista, K., Weinrich, S., Sträuber, H., Nikolausz, M., Nelles, M., Stinner, W., 2016. Optimization of hydrolysis and volatile fatty acids production

from sugarcane filter cake: Effects of urea supplementation and sodium hydroxide pretreatment. Bioresour. Technol. 199, 235–244. https://doi.org/10.1016/j.biortech.2015.07.117

Jiang, W.E.N., Kim, B.Y.S., Rutka, J.T., Chan, W.C.W., 2008. Nanoparticle-mediated cellular response is size-dependent 145–150. https://doi.org/10.1038/nnano.2008.30

Kang, Y.R., Su, Y., Wang, J., Chu, Y.X., Tian, G., He, R., 2021. Effects of different pretreatment methods on biogas production and microbial community in anaerobic digestion of wheat straw. Environ. Sci. Pollut. Res. https://doi.org/10.1007/s11356-021-14296-5

Krongthamchat, K., Riffat, R., Dararat, S., 2006. Effect of trace metals on halophilic and mixed cultures in anaerobic treatment. Int. J. Environ. Sci. Technol. 3, 103–112. https://doi.org/10.1007/BF03325913

Lee, Y.J., Lee, D.J., 2019. Impact of adding metal nanoparticles on anaerobic digestion performance – A review. Bioresour. Technol. 292, 121926. https://doi.org/10.1016/j.biortech.2019.121926

Li, Z., Wachemo, A.C., Yuan, H., Korai, R.M., Li, X., 2020. Improving methane content and yield from rice straw by adding extra hydrogen into a two-stage anaerobic digestion system. Int. J. Hydrogen Energy 45, 3739–3749. https://doi.org/10.1016/j.ijhydene.2019.07.235

Mamani, J.B., Gamarra, L.F., 2014. Synthesis and Characterization of Fe 3 O 4 Nanoparticles with Perspectives in Biomedical Applications 17, 542–549.

Moraes, B.S., Junqueira, T.L., Pavanello, L.G., Cavalett, O., Mantelatto, P.E., Bonomi, A., Zaiat, M., 2014. Anaerobic digestion of vinasse from sugarcane biorefineries in Brazil from energy, environmental, and economic perspectives: Profit or expense?

Appl. Energy 113, 825–835. https://doi.org/10.1016/j.apenergy.2013.07.018

Moraes, B.S., Zaiat, M., Bonomi, A., 2015. Anaerobic digestion of vinasse from sugarcane ethanol production in Brazil: Challenges and perspectives. Renew. Sustain. Energy Rev. 44, 888–903. https://doi.org/10.1016/j.rser.2015.01.023

Mu, H., Chen, Y., Xiao, N., 2011a. Bioresource Technology Effects of metal oxide nanoparticles (TiO 2 , Al 2 O 3 , SiO 2 and ZnO) on waste activated sludge anaerobic digestion. Bioresour. Technol. 102, 10305–10311. https://doi.org/10.1016/j.biortech.2011.08.100

Mu, H., Chen, Y., Xiao, N., 2011b. Effects of metal oxide nanoparticles (TiO 2, Al 2O 3, SiO 2 and ZnO) on waste activated sludge anaerobic digestion. Bioresour. Technol. 102, 10305–10311. https://doi.org/10.1016/j.biortech.2011.08.100

Ni, S.Q., Ni, J., Yang, N., Wang, J., 2013. Effect of magnetic nanoparticles on the performance of activated sludge treatment system. Bioresour. Technol. 143, 555–561. https://doi.org/10.1016/j.biortech.2013.06.041

Owusu-Agyeman, I., Plaza, E., Cetecioglu, Z., 2020. Production of volatile fatty acids through co-digestion of sewage sludge and external organic waste: Effect of substrate proportions and long-term operation. Waste Manag. 112, 30–39. https://doi.org/10.1016/j.wasman.2020.05.027

Peng, X., Börner, R.A., Nges, I.A., Liu, J., 2014. Impact of bioaugmentation on biochemical methane potential for wheat straw with addition of Clostridium cellulolyticum. Bioresour. Technol. 152, 567–571. https://doi.org/10.1016/j.biortech.2013.11.067

Ripley, L.E., Boyle, W.C., Converse, J.C., 1986. Improved alkalimetric monitoring for anaerobic digestion of high-strength waste.

Romero-Güiza, M.S., Vila, J., Mata-Alvarez, J., Chimenos, J.M., Astals, S., 2016. The

role of additives on anaerobic digestion: A review. Renew. Sustain. Energy Rev. 58, 1486–1499. https://doi.org/10.1016/j.rser.2015.12.094

Scherer, P., Lippert, H., Wolff, G., 1983. Composition of the major elements and trace elements of 10 methanogenic bacteria determined by inductively coupled plasma emission spectrometry. Biol. Trace Elem. Res. 5, 149–163. https://doi.org/10.1007/BF02916619

Schnürer, A., Zellner, G., Svensson, B.H., 1999. Mesophilic syntrophic acetate oxidation during methane formation in biogas reactors. FEMS Microbiol. Ecol. 29, 249–261. https://doi.org/10.1016/S0168-6496(99)00016-1

Sh, U., 2010. Mineral Requirements for Mesophilic and Thermophilic Archive of SID. Arch. SID 4, 33–40.

Triolo, J.M., Pedersen, L., Qu, H., Sommer, S.G., 2012. Biochemical methane potential and anaerobic biodegradability of non-herbaceous and herbaceous phytomass in biogas production. Bioresour. Technol. 125, 226–232. https://doi.org/10.1016/j.biortech.2012.08.079

VDI 4630, 2006. Fermentation of organic materials. Characterization of the substrate, sampling, collection of material data, fermentation tests. Düsseldorf: Verein Deutscher Ingenieure.

Volpi, M.P.C., Brenelli, L.B., Mockaitis, G., Rabelo, S.C., Franco, T.T., Moraes, B.S., 2021a. Use of lignocellulosic residue from second-generation ethanol production to enhance methane production through co-digestion. Bioenergy Res. https://doi.org/10.1007/s12155-021-10293-1

Volpi, M.P.C., Junior, A.D.N.F., Franco, T.T., Moraes, B.S., 2021b. Operational and biochemical aspects of co-digestion (co-AD) from sugarcane vinasse, filter cake, and deacetylation liquor. Appl. Microbiol. Biotechnol.

https://doi.org/10.1007/s00253-021-11635-x

Vongvichiankul, C., Deebao, J., Khongnakorn, W., 2017. Relationship between pH, Oxidation Reduction Potential (ORP) and Biogas Production in Mesophilic Screw Anaerobic Digester. Energy Procedia 138, 877–882. https://doi.org/10.1016/j.egypro.2017.10.113

Wang, P., Wang, H., Qiu, Y., Ren, L., Jiang, B., 2018. Microbial characteristics in anaerobic digestion process of food waste for methane production–A review. Bioresour. Technol. 248, 29–36. https://doi.org/10.1016/j.biortech.2017.06.152

Wang, T., Zhang, D., Dai, L., Chen, Y., Dai, X., 2016. Effects of metal nanoparticles on methane production from waste-activated sludge and microorganism community shift in anaerobic granular sludge. Sci. Rep. 6, 1–10. https://doi.org/10.1038/srep25857

Wang, Y., Zhang, Y., Wang, J., Meng, L., 2009. Effects of volatile fatty acid concentrations on methane yield and methanogenic bacteria. Biomass and Bioenergy. https://doi.org/10.1016/j.biombioe.2009.01.007

Wiegant, W.M., Hennink, M., Lettinga, G., 1986. Separation of the propionate degradation to improve the efficiency of thermophilic anaerobic treatment of acidified wastewaters. Water Res. 20, 517–524. https://doi.org/https://doi.org/10.1016/0043-1354(86)90202-2

Wu, X., Tian, Z., Lv, Z., Chen, Z., Liu, Y., Yong, X., Zhou, J., Xie, X., Jia, H., Wei, P., 2020. Effects of copper salts on performance, antibiotic resistance genes, and microbial community during thermophilic anaerobic digestion of swine manure. Bioresour. Technol. 300, 122728. https://doi.org/10.1016/j.biortech.2019.122728

Xie, S., Li, X., Wang, C., Kulandaivelu, J., Jiang, G., 2020. Enhanced anaerobic digestion of primary sludge with additives: Performance and mechanisms.

Bioresour. Technol. 316, 123970. https://doi.org/10.1016/j.biortech.2020.123970

Yu, B., Lou, Z., Zhang, D., Shan, A., Yuan, H., Zhu, N., Zhang, K., 2015. Variations of organic matters and microbial community in thermophilic anaerobic digestion of waste activated sludge with the addition of ferric salts. Bioresour. Technol. 179, 291–298. https://doi.org/10.1016/j.biortech.2014.12.011

Zhang, L., Gong, X., Wang, L., Guo, K., Cao, S., Zhou, Y., 2021. Metagenomic insights into the effect of thermal hydrolysis pre-treatment on microbial community of an anaerobic digestion system. Sci. Total Environ. 791, 148096. https://doi.org/10.1016/j.scitotenv.2021.148096

Zhang, W., Wu, S., Guo, J., Zhou, J., Dong, R., 2015. Performance and kinetic evaluation of semi-continuously fed anaerobic digesters treating food waste: Role of trace elements. Bioresour. Technol. 178, 297–305. https://doi.org/10.1016/j.biortech.2014.08.046

Zhang, Y., Jing, Y., Zhang, J., Sun, L., Quan, X., 2011. Performance of a ZVI-UASB reactor for azo dye wastewater treatment. J. Chem. Technol. Biotechnol. 86, 199–204. https://doi.org/10.1002/jctb.2485

Zhang, Y., Zhang, Z., Suzuki, K., Maekawa, T., 2003. Uptake and mass balance of trace metals for methane producing bacteria. Biomass and Bioenergy 25, 427–433. https://doi.org/10.1016/S0961-9534(03)00012-6

Zhang, Z., Guo, L., Wang, Y., Zhao, Y., She, Z., Gao, M., Guo, Y., 2020. Application of iron oxide (Fe3O4) nanoparticles during the two-stage anaerobic digestion with waste sludge: Impact on the biogas production and the substrate metabolism. Renew. Energy 146, 2724–2735. https://doi.org/10.1016/j.renene.2019.08.078

Zhu, X., Blanco, E., Bhatti, M., Borrion, A., 2021. Impact of metallic nanoparticles on anaerobic digestion: A systematic review. Sci. Total Environ. 757.

https://doi.org/10.1016/j.scitotenv.2020.143747